Backscattering from small-scale breaking wave turbulence structure generated by FLUENT*

Luo Gen(罗 根) and Zhang Min(张 民)†

School of Physics and Optoelectronic Engineering, Xidian University, Xi'an 710071, *China*

(Received 25 March 2014; revised manuscript received 22 May 2014; published online 10 October 2014)

A breaking wave can exert a great influence on the electromagnetic (EM) scattering result from sea surfaces. In this paper, the process of small-scale wave breaking is simulated by the commercial computational fluid dynamics (CFD) software FLUENT, and the backscattering radar cross section (RCS) of the turbulence structure after breaking is calculated with the method of moments. The scattering results can reflect the turbulent intensities of the wave profiles and can indicate high polarization ratios at moderate incident angles, which should be attributed to the incoherent backscatter from surface disturbance of turbulence structure. Compared with the wave profile before breaking, the turbulence structure has no obvious geometrical characteristic of a plunging breaker, and no sea spikes are present at large incident angles either. In summary, the study of EM scattering from turbulence structure can provide a basis to explain the anomalies of EM scattering from sea surfaces and help us understand the scattering mechanism about the breaking wave more completely.

Keywords: FLUENT, turbulence structure, EM scattering, high polarization ratios

PACS: 41.20.Jb, 41.20.–q, 47.27.E– **DOI:** 10.1088/1674-1056/23/12/124101

1. Introduction

Scientists have been dedicated to the study of EM scattering from sea surfaces, and many methods have been proposed. The two-scale method (TSM) based on the Bragg scattering may be the most preferable one, which can well describe the scattering of sea surfaces at moderate incidence angles.[1–4] However, scattering signatures from high-resolution radar are not consistent with those from the TSM at large incident angles, which represent strong backscatter events (sea spikes), polarization ratios exceeding 0 dB or even 10 dB.[5,6] Also, sea spikes are evident in moderate incident angle measurements according to some other published research results.[7,8] All the phenomena cannot be explained by the traditional scattering theory.

The non-Bragg scattering from a breaking wave is usually considered as the main reason for discrepancies between the theoretical results and the measured data. There are some approximation and numerical models[9–16] for the breaking wave which have been used to explain the discrepancies between the published research results. In the above models, only the LONGTANK series in Refs. [12]–[14] is strictly generated by the numerical method. The numerical method can describe the breaking wave relatively accurately and give reliable scattering results of the breaking wave compared with the approximation models. Holliday *et al.*[12] have studied the backscattering from the breaking waves of LONGTANK series at X band. The results indicated that the breaking waves could give rise to sea spikes at large incident angles, and no sea spikes were exhibited at the moderate incident angle of 40°. Also, West,[13] West and Zhao[14] have described the scattering mechanisms of multipath scattering and direct scattering from LONGTANK series, and the results indicated that they could both give rise to sea spikes and high polarization ratios at large incident angles. However, there are few studies of EM scattering from the turbulence structure after breaking, and it is necessary to make some analyses of the scattering of turbulence structure.

The development of computer technology makes it possible to simulate many kinds of breaking waves and the turbulence structures after breaking by employing the CFD methods. Recently one- or two-dimensional breaking waves have been simulated with CFD methods,[17–19] and the turbulence structures after breaking have also been analyzed. The results from the CFD methods are relatively reliable, although the simulated wave profiles have some differences from the real situation results. It is of significance to introduce the breaking waves and turbulence structures after breaking established by CFD methods for the study of EM scattering from the complex and nonlinear breaking waves.

The commercial CFD software FLUENT can be used to calculate the problems of fluid mechanics. This software is convenient to the one who has the knowledge of the software, and it had been used to calculate the problem of ship wakes.[20] In this paper, we use FLUENT to simulate the whole process of small-scale wave breaking. The turbulence structure after

*Project supported by the National Natural Science Foundation of China (Grant Nos. 61372004 and 41306188), the Fundamental Research Funds for the Central Universities, China (Grant No. K 5051207015), and the Foundation of the Science and Technology on Electromagnetic Scattering Laboratory, China (Grant No. HX0113071414).

†Corresponding author. E-mail: mzhang@mail.xidian.edu.cn

© 2014 Chinese Physical Society and IOP Publishing Ltd

breaking can be obtained, which is similar to the results in Refs. [17]–[19]. Using the method of moments, the backscattering coefficients of the turbulence structure generated by FLUENT at all incident angles are calculated. The scattering results can reflect the turbulent intensities of the wave profiles, and high polarization ratios are exhibited at moderate incident angles, which should be attributed to the incoherent backscatter from surface disturbances of turbulence structure. The wave profile after breaking has no obvious geometrical characteristics, which is similar to the case of the wave profile before breaking, so no sea spikes are present at large incident angles either.

The rest of this paper is organized as follows. In Section 2, the turbulence structure is generated by FLUENT. Backscattering from the turbulence structure with the method of moments is introduced in Section 3. The backscattering coefficients of the turbulence structure are calculated at different incident angles in Section 4. Finally some conclusions are drawn and the brief discussion is presented in Section 5.

2. Generation of turbulence structure by FLUENT

The computational model is shown in Fig. 1, where the boundary *AD* represents the moving boundary, the boundary *DC* is the wave flume bottom, the boundary *BC* is the end of the wave flume, the boundary *AB* is the top of the flume, the *ED* is the water depth at the initial time, which is set to be half the length of *AD* in our simulations, the boundaries *AD*, *DC*, and *BC* are walls, while the boundary *AB* is pressure inlet. Owing to the fact that the total computational time is short (less than 3.0 seconds) and the dominant wave does not propagate to the boundary *BC*, we do not set a wave absorbing zone at the end of the wave flume either. To implement the movement of the moving boundary *AD*, the user-define-function (UDF) is employed. The volume of fluid (VOF) is used to deal with the surface flow, and the surface tension is chosen to be 0.074 N/m. An example of the breaking wave generated by FLUENT is also shown in Fig. 1, the part with oblique lines represents water, and the above part denotes air.

The velocity of the moving boundary *AD* is described as follows:

$$U = a\omega \sin \omega t, \tag{1}$$

where a is the stroke of the moving boundary, t is the running time, and ω is the angular frequency. The displacement of the paddle is

$$S_\omega = -a\cos \omega t + a. \tag{2}$$

Because the water in the flume is static at the initial time, the wave maker can make the velocities of the water particles different, and then the wave becomes curled and broken. After breaking, the turbulence structures can be obtained.

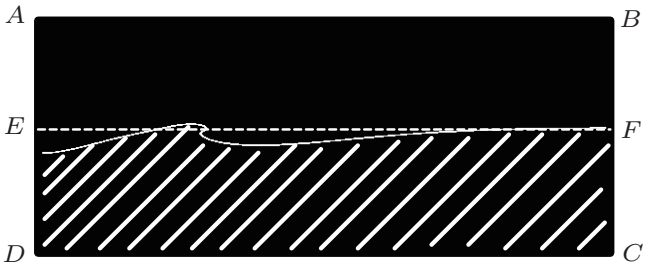


Fig. 1. Computational model and example of the breaking wave.

Table 1. Parameters of the waves.

a/m	*ω*/(rad/s)	*AB*/m	*AD*/m
0.075	8.5	6	1

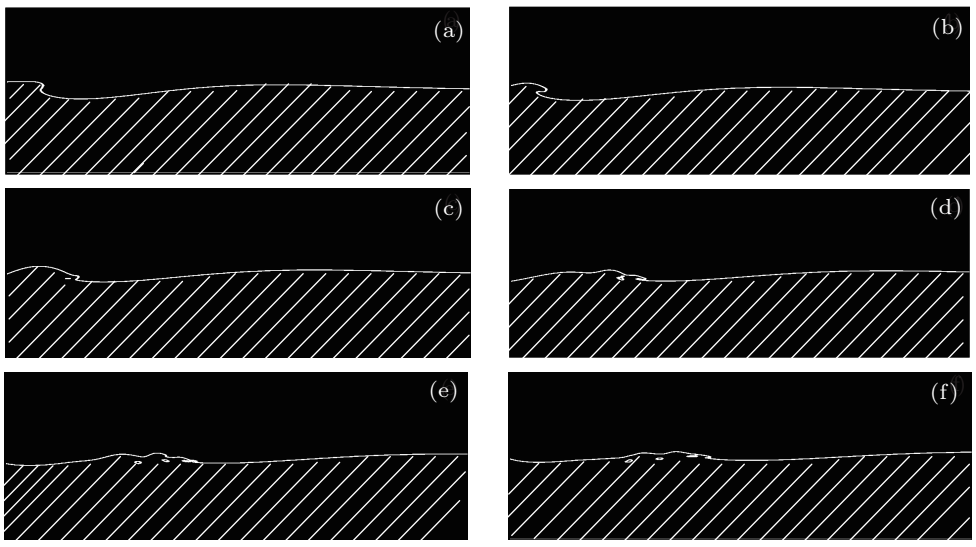


Fig. 2. Process of wave breaking.

In this paper, the parameters of the simulated wave are listed in Table 1, and more kinds of waves can be simulated by defining different values of ω and a. There are 1.2×10^5 rectangular cells for the computational area, the interval count for AB is 600 and AD is 200. In order to simulate the process of wave breaking, the RNG k–ε viscous model is used to deal with the problem. The time step $\mathrm{d}t = 0.005$ s is employed at the stage of before breaking, and $\mathrm{d}t$ is chosen to be 0.002 s when the wave is about to be broken for better observation of the breaking wave. For more detailed information about the operation, readers can refer to Ref. [21].

Taking all the things into account, the breaking wave and turbulence structure can be obtained. Figure 2 shows the whole process of wave breaking. Figure 2(a) shows the wave becoming steep, and figure 2(b) displays the wave being seriously plunging. Figure 2(c) shows the wave starting to break, and figures 2(d)–2(f) present the initial, intermediate, and later stages of the turbulence structures after breaking, respectively. In the following sections, we use the method of moments to study the EM scattering of the turbulence structure.

3. Backscattering from the turbulence structure with method of moments

The geometry of the scattering process is illustrated in Fig. 3, where θ_i denotes the incident angle, $\boldsymbol{k}_\mathrm{i}$ is the incident wave vector, and $\boldsymbol{k}_\mathrm{s}$ is the scattering wave vector. The method of moments or other similar fast numerical algorithm can be used to calculate the EM scattering from the rough surface, and the problem of a target above or below the rough surface can be considered as a dielectric surface. Some similar practices have been done in Refs. [22]–[24]. For the turbulence structure, the surfaces are assumed to be perfect electric conductors (PEC), and all calculations are performed in the one-dimensional space. Based on the solution of the magnetic field integral equation (MFIE) for the surface current J, the exact numerical calculations can be performed. The scattering field in the far-field can be calculated as

$$\varphi^s(\theta_\mathrm{s},r,\theta_\mathrm{i})=\frac{\exp(-\mathrm{j}kr)}{\sqrt{r}}\int Q(x,\theta_\mathrm{s})J(x;\theta_\mathrm{i})\,\mathrm{d}x, \tag{3}$$

where θ_i is the incident angle, θ_s is the scattering angle (for the backscattering case, $\theta_\mathrm{s}=-\theta_\mathrm{i}$), k is the wavenumber of the incident wave, r is the distance from the turbulence structure to the radar receiver, and Q is dependent on the polarization. For horizontal polarization, Q can be expressed as[22]

$$\begin{aligned}Q(x,\theta_\mathrm{s}) &= \frac{\mathrm{e}^{-\mathrm{j}\pi/4}}{2\sqrt{2\pi k}}(-\exp\{\mathrm{j}k[x\sin\theta_\mathrm{s}+y\cos\theta_\mathrm{s}]\}\\ &\quad\times\sqrt{1+y_x^2}).\end{aligned} \tag{4}$$

In the case of vertical polarization, Q is

$$\begin{aligned}Q(x,\theta_\mathrm{s}) &= \frac{\mathrm{e}^{-\mathrm{j}\pi/4}}{2\sqrt{2\pi k}}(\mathrm{j}k[-y_x\sin\theta_\mathrm{s}+\cos\theta_\mathrm{s}]\\ &\quad\times\exp\{\mathrm{j}k[x\sin\theta_\mathrm{s}+y\cos\theta_\mathrm{s}]\}).\end{aligned} \tag{5}$$

Suppose that a tapered wave is incident on the sea surface and can be expressed as[23,25]

$$\varphi_\mathrm{i}(x,y) = G(x,y,\theta_\mathrm{i})\exp[-\mathrm{j}k(x\sin\theta_\mathrm{i}-y\cos\theta_\mathrm{i})], \tag{6}$$

$$\begin{aligned}G(x,y,\theta_\mathrm{i}) &= \exp\left[-\frac{(x+y\tan\theta_\mathrm{i})^2}{v^2}-\mathrm{j}\frac{k(x\sin\theta_\mathrm{i}-y\cos\theta_\mathrm{i})}{(kv\cos\theta_\mathrm{i})^2}\right.\\ &\quad\left.\times\left(\frac{2(x+y\tan\theta_\mathrm{i})^2}{v^2}-1\right)\right],\end{aligned} \tag{7}$$

where $G(x,y)$ is the taper function and v is the parameter that controls the beam waist. In this paper, the parameter v is selected to be one-fourth of the size of computation area. Then the normalized radar cross section for a particular surface can be defined as[26]

$$\sigma^0(\theta_\mathrm{s},\theta_\mathrm{i})=\lim_{r\to\infty}\frac{2\pi r|\varphi^\mathrm{s}|^2}{\int|\varphi^\mathrm{i}(x,0)|^2\,\mathrm{d}x}. \tag{8}$$

So the backscattering coefficient of the turbulence structure can be calculated. Here, the point-matching method is employed for the method of moments, so the testing function is Dirac function and the basis function is pulse basis function. For the method of moments, we let the maximal sample interval be less than or equal to $\lambda/10$, where λ is the incident wavelength. In the high frequency bands, the wavelength of the incident wave should be relatively short, and the simulated model might not meet the above requirement. To make the maximal sample interval less than or equal to $\lambda/10$, the method of linear interpolation is employed to deal with the simulated data. In this way, we can make the simulated model able to be calculated by the method of moments for high frequency bands.

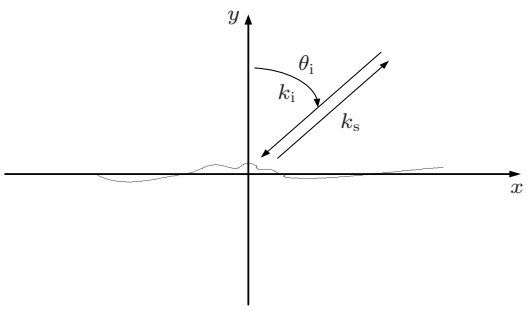


Fig. 3. Geometry of the turbulence structure scattering model.

4. Numerical results

First, we calculate the backscattering coefficients of the wave profile before breaking; the wave profile in Fig. 2(a) is

employed. Figure 4(a) is the geometry model of the steep wave profile, and figures 4(b)–4(d) show the backscattering coefficients at frequencies at 10 GHz, 12 GHz, and 15 GHz respectively. The center of the turbulence structure is set to be at the origin of coordinate for each profile, and the computation area ranges from −0.6 m to 0.6 m. For traditional sea surface, scattering coefficients will become relatively small at large incident angles, especially for HH polarization. Also, polarization ratios (HH/VV) are usually less than 0 dB at moderate incident angles and −20 dB at large incident angles.[3,4] From Fig. 4, we can see that the scattering coefficients of a steep wave profile can reach big values at large incident angles, and the results of HH polarization can be larger than those of VV polarization at some incident angles. Compared with traditional results, these are the typical phenomena of sea spikes and high polarization ratios at large incident angles, which are consistent with the scattering results of LONGTANK series in Refs. [12]–[14].

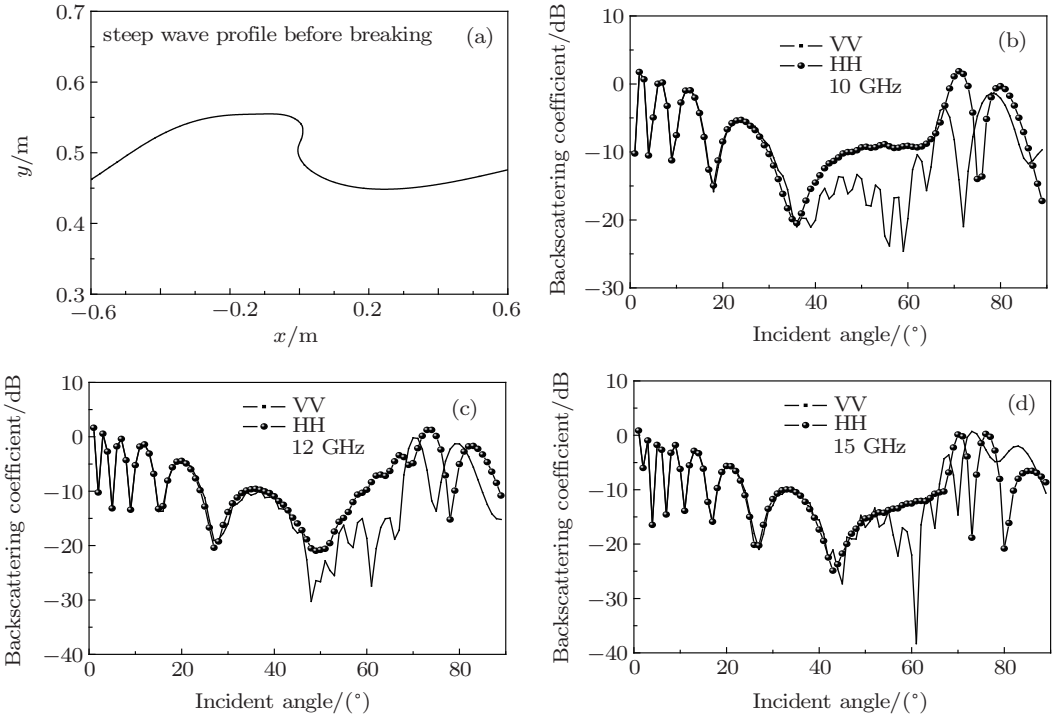


Fig. 4. Steep wave profile before breaking (a), and backscattering coefficients of the wave profiles before breaking versus incident angle at frequencies of 10 GHz (b), 12 GHz (c), and 15 GHz (d).

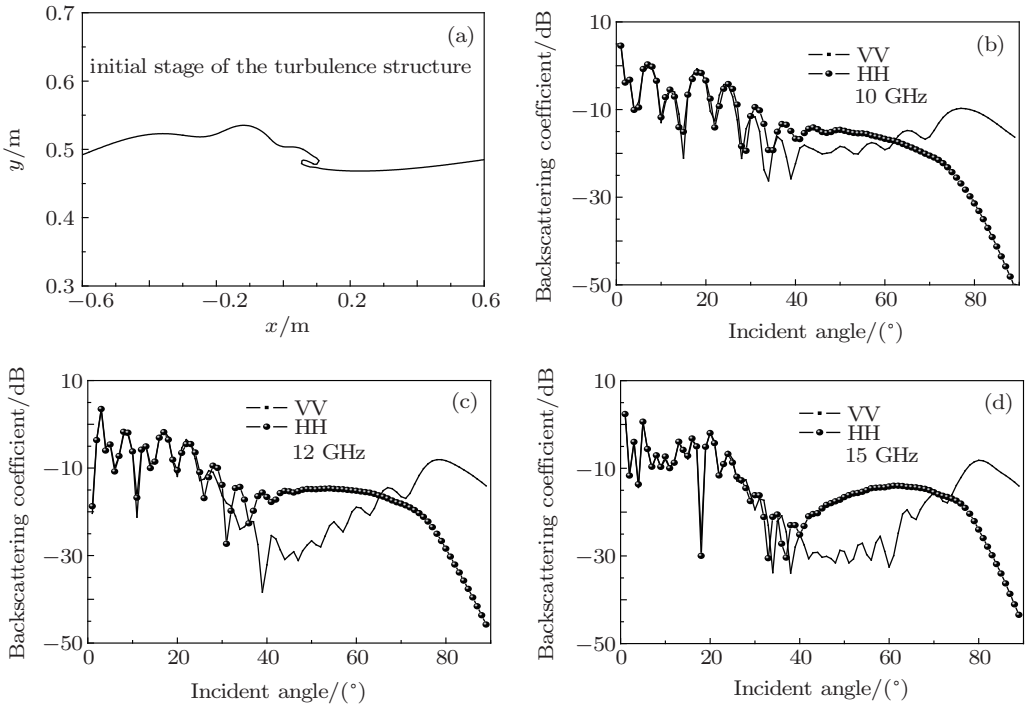


Fig. 5. Wave profile of turbulence structure at the initial stage (a) and backscattering coefficients of the turbulence structure at initial stage versus incident angle at frequencies of 10 GHz (b), 12 GHz (c), and 15 GHz (d).

Then backscattering coefficients of the turbulence structure versus incident angle are calculated. The computation conditions are similar to those of the wave profile before breaking. Figure 5(a) shows the geometry model of initial stage of the turbulence structure, figures 5(b)–5(d) show the scattering results at frequencies of 10 GHz, 12 GHz, and 15 GHz respectively. Figures 6 and 7 are similar to Fig. 5, which show the results of the intermediate and later stages of the turbulence structures. From Fig. 5, we can see that the scattering coefficients of the initial stage of the turbulence structure oscillate with incident angle. The oscillation becomes stronger when the turbulence structure enters into the intermediate stage (see Fig. 6), and the oscillation becomes gentle at the later stage according to Fig. 7. These results just reflect the turbulent intensities of the wave profiles. At the initial stage, the wave profile is not very turbulent, so the oscillation of the backscattering coefficients with the incident angle is not very strong. When the wave profile enters into the intermediate stage, the turbulence becomes very turbulent, and scattering coefficients oscillate seriously with the incident angle. Entering into the later stage, the turbulence of the wave profile becomes weak, and the oscillations of scattering results become gentle. Also, we can see the backscattering coefficients of HH polarization can be larger than those of VV polarization at moderate incident angles for the turbulence structure, which could be treated as a kind of super-event, although there are no obvious geometrical characteristics of a plunging breaker as the scenario of the wave profile before breaking.

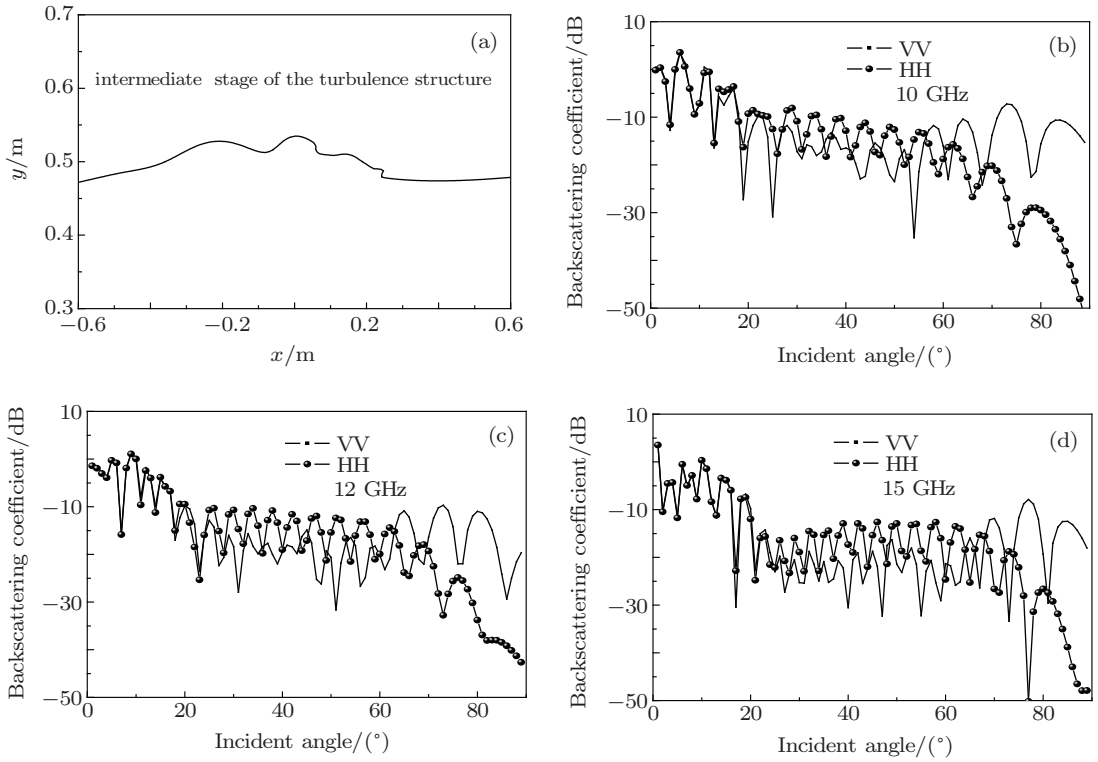


Fig. 6. Wave profile of turbulence structure at the later stage (a) and backscattering coefficients of intermediate stage of the turbulence structure versus incident angles at frequencies of 10 GHz (b), 12 GHz (c), and 15 GHz (d).

Similarly, Ericson *et al.*[27] and Walker *et al.*[28] have studied the radar backscatter of stationary breaking waves experimentally. The stationary breaking waves were generated by submerging a stationary hydrofoil in a uniform flow, which could be considered as another kind of turbulence to some degree. *X* band radar backscatter measurements were made along the stationary breaking waves for a moderate incident angle of 45°. The measurement could present sea spikes and high polarizations at the positions near the breaking crest for an incident angle of 45°. For the stationary breaking wave in Refs. [27] and [28], there existed neither wedge-like wave nor other sharp wave. The total field is usually given by the sum of the coherent and incoherent fields. The total scattering cross-section σ is decomposed into a coherent component σ_{C} and an incoherent component σ_{I}. Traditionally, the coherent component σ_{C} is important at small incident angles. For moderate and large incident angles, σ_{C} will decay quickly and σ_{I} will be the main component. So Ericson and Walker *et al.* concluded that the incoherent backscatter from surface disturbances produced by breaking waves can account for the high radar returns or sea spikes at moderate incident angle. In the present paper, the EM scattering from the turbulence structure after breaking is studied. The scattering results obtained from the three stages of the turbulent structures can reflect the

turbulent intensities of the wave profiles, and high polarization ratios are exhibited at moderate incident angles. In addition, the high polarization ratios shift toward large incident angles as frequency becomes higher. Compared with the wave profile before breaking, the turbulence structure has no obvious geometrical characteristics of plunging breaker, and nor do the sea spikes appear at large incident angles. So, all the scattering phenomena should be attributed to the incoherent backscatter from surface disturbances of turbulence structure, which is similar to the scenarios in Refs. [27] and [28]. Generally speaking, the scattering results obtained from turbulence structure are different from those in cases of the traditional sea surfaces and the wave profile before breaking, and the study of EM scattering from turbulence structure can provide a basis to explain the anomalies of EM scattering from sea surfaces and help us understand the scattering mechanism for the breaking wave more completely.

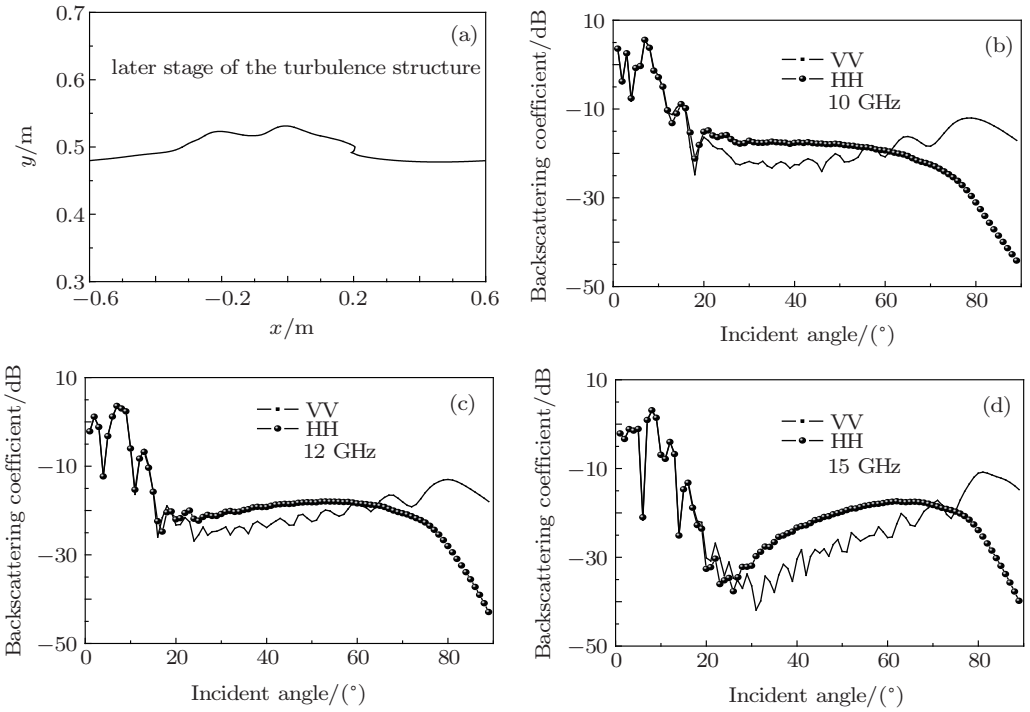


Fig. 7. Wave profile of turbulence structure at the later stage (a) and backscattering coefficients of later stage of the turbulence structure at later stage versus incident angle at frequencies of 10 GHz (b), 12 GHz (c), and 15 GHz (d).

5. Conclusions

In this paper, the EM scattering from turbulence structure after breaking is studied. The whole process of small-scale wave breaking is simulated by FLUENT and the turbulence structures at different stages are obtained. Using the method of moments, the backscattering coefficients of turbulence structure are calculated. The scattering results can reflect the turbulent intensities of the wave profiles. The scattering coefficients oscillate seriously with the incident angle as the turbulence is very turbulent for the intermediate stage, and the scattering results become relatively gentle at the initial and later stages as the turbulences of the wave profiles are weaker than at the intermediate stage. Also, the backscattering coefficients of the turbulence structure can indicate high polarization ratios and give rise to super-events at moderate incident angles, although there is no obvious geometrical characteristic of a plunging breaker before breaking. All the scattering results should be attributed to the incoherent backscatter from surface disturbances from turbulence structure. In conclusion, the EM scattering result obtained from a turbulence structure can provide a basis to explain the anomalies of EM scattering from sea surfaces and help us understand the scattering mechanism for the breaking wave more completely. Although the turbulence structure in this paper is simple, it is sufficient enough to indicate the mechanism for the incoherent backscatter scattering from turbulence structure. In future work, we will establish more complex turbulence structure for better understanding the EM scattering from the breaking wave and turbulence.

References

[1] Wright J W 1968 *IEEE Trans. Anten. Propag.* **AP-16** 217
[2] Mouche A A, Chapron B and Reul N 2007 *Waves in Random and Complex Media* **17** 321
[3] Nie D and Zhang M 2010 *Chin. Phys. B* **19** 074101
[4] Zhang Y D and Wu Z S 2002 *Chin. Phys. Lett.* **19** 666
[5] Liu Y, Frasier S and McIntosh R 1998 *IEEE Trans. Anten. Propag.* **46** 27

[6] Hwang P A, Sletten M A and Toporkov J V 2008 *J. Geophys. Res.* **113** C02003
[7] Jessup A T, Keller W C and Melville W K 1990 *J. Geophys. Res.* **95** 9679
[8] Jessup A T and Melville W K 1991 *J. Geophys. Res.* **96** 20547
[9] Kalmykov A I and Pustovoytenko V V 1976 *J. Geophys. Res.* **81** 1960
[10] Lyzenga D R, Maffett A L and Shuchman R A 1983 *IEEE Trans. Geosci. Remote Sens.* **GE-21** 502
[11] Kudryavtsev V, Hauser D, Caudal G and Chapron B 2003 *J. Geophys. Res.* **108** FET 2-1
[12] Holliday D, DeRaad L L and St-Cyr G J 1998 *IEEE Trans. Anten. Propag.* **46** 108
[13] West J C 2002 *IEEE Trans. Geosci. Remote Sens.* **40** 523
[14] West J C and Zhao Z Q 2002 *IEEE Trans. Geosci. Remote Sens.* **40** 583
[15] Liu Y, Wei E B, Hong J L and Ge Y 2006 *Chin. Phys.* **15** 2175
[16] Liang Y and Guo L X 2009 *Acta Phys. Sin.* **58** 6158 (in Chinese)
[17] Sambe A N, Sous D, Golay F, Fraunie P and Marcer R 2011 *Eur. J. Mech. B: Fluids* **30** 577
[18] Lubin P, Glockner S, Kimmoun O and Branger H 2011 *Eur. J. Mech. B: Fluids* **30** 552
[19] Lakehal D and Liovic P 2011 *J. Fluid Mech.* **674** 522
[20] Fujimura A, Soloviev A and Kudryavtsev V 2010 *IEEE Geosci. Remote Sens. Lett.* **7** 646
[21] 2006 *Fluent User's Guide* (Fluent Inc. Lebanon NH)
[22] Toporkov J V, Marchand R T and Brown G S 1998 *IEEE Trans. Anten. Propag.* **46** 150
[23] An Y Y, Wang D X and Chen R S 2013 *Electromagnetics* **33** 10
[24] An Y Y and Chen R S 2012 *Appl. Comput. Electromag.* **27** 541
[25] Tsang L, Kong J A and Ding K H 2001 *Scattering of Electromagnetic Waves* (New York: John Wiley & Sons Inc.) p. 119
[26] Toporkov J V and Brown G S 2002 *IEEE Trans. Anten. Propag.* **50** 417
[27] Ericson E A, Lyzenga D R and Walker D T 1999 *J. Geophys. Res.* **104** 29679
[28] Walker D T, Lyzenga D R, Ericson E A and Lund D E 1996 *Proc. R. Soc. London, Ser. A* **452** 1953